Crystal Structure of Rabbit Phosphoglucose Isomerase Complexed with 5-Phospho-D-Arabinonate Identifies the Role of Glu357 in Catalysis‡

Constance J. Jeffery,*,# Renaud Hardré,§ and Laurent Salmon§

Laboratory for Molecular Biology, MC567, Department of Biology, University of Illinois at Chicago, Chicago, Illinois 60607, USA, and Laboratoire de Chimie Bioorganique et Bioinorganique, CNRS-FRE 2127, Institut de Chimie Moléculaire d'Orsay, Bât. 420, Université Paris-XI, 91405 Orsay, France

Received August 7, 2000; Revised Manuscript Received November 24, 2000

ABSTRACT: Phosphoglucose isomerase (PGI; E.C. 5.3.1.9) catalyzes the second step in glycolysis, the interconversion of D-glucose-6-phosphate and D-fructose-6-phosphate. We determined the X-ray crystal structure of rabbit PGI complexed with a competitive inhibitor of isomerase activity, 5-phospho-D-arabinonate (5PAA), at 1.9 Å resolution. 5PAA is a better mimic of the proposed *cis*-enediol(ate) intermediate than 6-phospho-D-gluconate, which was used in a previously reported crystal structure of rabbit PGI. The orientation of 5PAA bound in the enzyme active site predicts that active site residue Glu357 is the residue that transfers a proton between C2 and C1 of the proposed *cis*-enediol(ate) intermediate. Amino acid residues Arg272 and Lys210 are predicted to be involved in stabilizing the negative charge of the intermediate.

Phosphoglucose isomerase (PGI; E.C. 5.3.1.9)[1] catalyzes the interconversion of D-glucose-6-phosphate (G6P) and D-fructose-6-phosphate (F6P). It is a key enzyme in glycolysis and gluconeogenesis and is required by nearly all organisms; exceptions include some obligate intracellular parasites such as Rickettsia (*1*).

Surprisingly, this cytosolic enzyme shares sequence identity to the extracellular cytokines and growth factors neuroleukin (NL) (*2*, *3*), autocrine motility factor (AMF) (*4*), and differentiation and maturation mediator (DMM) (*5*). Neuroleukin has been shown to promote the survival of some embryonic neurons and cause premature B cells to differentiate into antibody secreting cells. AMF affects the motility of tumor cells and may play a role in cancer metastasis and invasion (*4*). DMM can cause the in vitro differentiation of human myeloid leukemia HL-60 cells to terminal monocytic cells (*5*).

PGI is a dimer with 557 amino acids per subunit. Extensive characterization of PGI enzymatic activity has led to a proposed multistep catalytic mechanism that involves general acid−base catalysis (*6*−*9*). Since G6P exists predominantly in its cyclic form in solution (*10*), it is believed that the enzyme first catalyzes opening of the hexose ring to yield the open chain form of G6P. The reaction proceeds through a *cis*-enediol(ate) intermediate with the double bond located between C1 and C2. An enzymic base transfers a proton between C2 and C1 of the intermediate to form the open-chain form of F6P.

Previous crystallographic studies of PGI include a partial structure of the pig enzyme (*11*, *12*) and structures of PGI from *Bacillus stearothermophilus* (*13*) and rabbit (*14*). Two additional structures of the *B. stearothermophilus* enzyme were reported during the preparation of this manuscript (*15*). Of the three bacterial PGI structures, one contains no bound ligand, and the other two contain bound inhibitors 5-phospho-D-arabinonate (5PAA) or N-bromoacetylethanolamine phosphate. However, the bacterial PGI structures were determined in the presence of 50 mM inorganic phosphate, a competitive inhibitor of isomerase catalytic activity. Since the inorganic phosphate is likely to compete for the binding site of the inhibitor's phosphate group, the orientation of the inhibitors in the crystal structures of the bacterial enzyme might not represent the orientation of the opened form of the substrate G6P (or F6P) bound in the active site of the enzyme.

The previously reported rabbit PGI structure also contained a bound competitive inhibitor of isomerase catalytic activity, 6-phospho-D-gluconate (6PGA). Since the rabbit PGI structure was determined in the absence of added inorganic phosphate, the 6PGA inhibitor is likely to be bound with its phosphate group in the correct position in the active site. However, the other end of the 6PGA inhibitor differs from the substrates because it contains an extra oxygen atom bound to C1 (Figure 1). Also, 6PGA is a rather weak competitive inhibitor of the F6P isomerization catalyzed by rabbit PGI, with $K_i = 43\ \mu M$ [K_m (F6P) = 100 μM] (*16*). Interactions observed between the C1 and C2 of the 6PGA inhibitor and the enzyme might not represent the interactions between C1 and C2 of the intermediate and the enzyme. While the rabbit PGI/6PGA complex structure is likely to represent the

‡ Coordinates for the structure of phosphoglucose isomerase complexed with the competitive inhibitor 5-phospho-D-arabinonate are deposited in the Protein Data Bank with the ID code 1G98.

* To whom correspondence should be addressed: C. Jeffery: cjeffery@uic.edu. Telephone: 312-996-3168. FAX: 312-413-2691.

University of Illinois at Chicago.

§ Institut de Chimie Moléculaire d'Orsay.

[1] PGI, phosphoglucose isomerase; PDB, protein data bank; AMF, autocrine motility factor; NL, neuroleukin; DMM, differentiation and maturation mediator; 6PGA, 6-phospho-D-gluconate; 5PAH, 5-phospho-D-arabinonhydroxamate; 5PAA, 5-phospho-D-arabinonate; TIM, triosephosphate isomerase.

10.1021/bi0018483 CCC: $20.00
Published on Web 01/20/2001

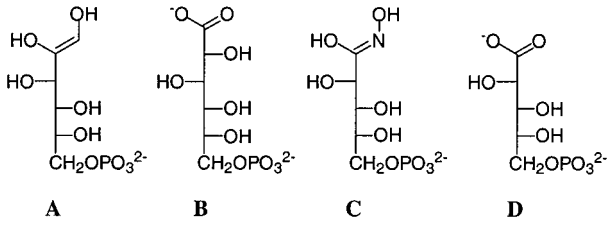

FIGURE 1: Proposed *cis*-enediol(ate) intermediate and inhibitor molecules mentioned in the text. (A**)** The 1,2-*cis*-enediol intermediate; (B**)** 6-phospho-D-gluconate; (C**)** 5PAH; **(**D**)** 5PAA.

correct binding of the phosphate end of the inhibitor/substrate, it is not clear which active site amino acid residues are involved in promoting proton transfer between C2 and C1.

Also, none of the structures reported so far have demonstrated a reason for the enzyme's strict specificity for the substrates G6P and F6P. Many phosphosugars, such as D-gluconate-6-phosphate (*17*), D-erythrose-4-phosphate (*18*), and other phosphorylated compounds, serve as competitive inhibitors of the reaction. However, other 6-carbon phosphosugars such as D-mannose-6-phosphate or D-galactose-6-phosphate are not substrates for the reaction. It might be expected that a crystal structure containing a compound more similar to the natural substrates than 6PGA would have additional interactions between the enzyme and the hydroxyl groups of the inhibitor that might play a role in enzyme specificity. To better understand the catalytic mechanism and substrate specificity of PGI, it would be good to have a structure of the enzyme with a good transition state mimic that was not solved in the presence of inorganic phosphate.

In addition, the highest resolution structures previously reported for rabbit and *B. stearothermophilus* PGI were solved at 2.5 to 2.3 Å resolution, respectively. We report herein the X-ray crystal structure of rabbit PGI with bound 5PAA inhibitor determined at 1.9 Å resolution.

MATERIALS AND METHODS

Crystallization of PGI. Rabbit skeletal muscle PGI was purchased from Sigma Chem. Co. The protein was desalted by ion exchange chromatography and concentrated as described previously (*14*). 5PAH was prepared as described previously (*19*). Crystals were grown by the hanging drop vapor diffusion method at room temperature. The hanging drops contained an equal mixture of protein solution [15−20 mg/mL PGI, 10 mM imidazole (pH 7.5), 50 mM KCl, 3 mM NaN_3, and 5 mM 5PAH] and reservoir solution [10−15% PEG 8000, 250 mM magnesium acetate, and 100 mM sodium cacodylate (pH 6.5)]. The drops were allowed to equilibrate with 1 mL of reservoir solution. The crystals were colorless hexagonal rods approximately $0.3 \times 0.3 \times 1.0$ mm^3 in size and with the symmetry of the orthorhombic space group $C222_1$ ($a = 82.83$ Å, $b = 116.55$ Å, $c = 271.82$ Å).

Data Collection and Structure Determination. Diffraction data from a single crystal of the enzyme−inhibitor complex, flash frozen at −180 °C, were collected at the APS beamline 14C (BioCars) at Argonne National Laboratories using monochromatic X-rays. Immediately before data collection, the crystal was soaked briefly in a stabilization solution containing 20% PEG 8000, 250 mM magnesium acetate, 100 mM sodium cacodylate (pH 6.5), and 5 mM 5PAH. The data set was processed with the programs DENZO and SCALEPACK (*20*).

Table 1: Statistics for Data Collection and Refinement[a]

data collection	PGI + 5PAA
space group	$C222_1$
cell dimensions (Å)	
a	82.83
b	116.55
c	271.82
temperature (° C)	−180
resolution limit (Å)	1.9
observed reflections	
total	486 988
unique	95 997
completeness (%)	94.3 (99.8)
redundancy	5.1
Rsym (% on I)[b]	0.035
refinement	
resolution range (Å)	8.0−1.9 (1.97−1.90)
R factor (%)	21.1(22.6)
R_{free} (%)[c]	23.6 (27.4)
ordered water molecules	892
r.m.s. deviations from ideal geometry	
bond lengths (Å)	0.0088
bond angles (°)	1.4
average B factor (Å^2)	26.0

[a] The numbers in parentheses correspond to the values for the last resolution bin of data. [b] Rsym = $\Sigma|I_i - \langle I\rangle|/\Sigma I_i$ R factor = $\Sigma||Fo| - |Fc||/\Sigma|Fo|$. [c] R_{free} is the equivalent of R factor, but it is calculated for 10% randomly chosen set of reflections that were omitted from the refinement process.

Refinement. Refinement consisted of alternating rounds of computational refinement using the CNS program package (*21*) and manual fitting of the model to the electron density maps using the program O (*22*). The initial model for refinement was the previously reported rabbit PGI structure (PDB entry 1DQR, *14*) after removal of all the water molecules and the inhibitor molecule. Ten percent of the data set was set aside to compute R_{free} (*23*). Simulated annealing was used to remove model bias. Data between 8 and 1.9 Å resolution were used in positional and individual B factor refinement. The "peak picking" feature of CNS was used to select about 400 water molecules for the structure based on electron density maps with coefficients |Fo − Fc|, together with criteria based on geometry and refined B-factors. Additional waters were placed using the ARPP subprogram in CCP4 (*24*). The inhibitor molecule was built into each of the two active sites in the PGI molecule. The final R factor is 21.1 for all data from 8 to 1.9 Å resolution with a free R factor of 23.6 (Table 1).

RESULTS AND DISCUSSION

The crystal structure of rabbit skeletal muscle PGI was solved at 1.9 Å resolution with a bound competitive inhibitor that mimics the proposed *cis*-enediol(ate) intermediate of the isomerization reaction. The highest resolution structures previously solved for the rabbit PGI and *B. stearothermophilus* PGI were determined at 2.5 Å and 2.3 Å resolution, respectively, so this new structure provides a clearer view of the active site. The PGI/5PAA final model includes two PGI subunits, two bound inhibitor molecules, and 892 water molecules per asymmetric unit. Each subunit in the model contains residues 1 through 555; the two amino acids at the C-terminus of each subunit were disordered.

The overall structure of the PGI protein in this model is similar to that reported previously for rabbit PGI with bound 6-phospho-D-gluconate inhibitor (*14*), except for a small conformational change described below. The root-mean-square deviation of alpha carbon positions for the two rabbit PGI structures is 0.60 Å. The two subunits in the asymmetric unit are arranged as a dimer. Each subunit is made up of one large and one small α/β sandwich domain and has an extended C-terminus containing two helices and a loop that extends across the surface of the other subunit in the dimer. The rms deviation of α carbon positions for the two subunits in the dimer is 0.33 Å.

Bound Inhibitor. A difference electron density map calculated with the coefficients |Fo − Fc| and contoured at 2.0 σ contains electron density corresponding to a bound inhibitor molecule in each of the two identical substrate binding pockets. These pockets correspond to the binding site for 6PGA in the rabbit PGI structure reported previously. The pockets are located between the two α/β sandwich domains of one subunit and at the interface between the two subunits and are composed of residues from both subunits of the dimer and from both domains of a subunit. For example, one active site includes amino acid residues 158, 271, 159, 518, 272, 357, and 209 through 211 from subunit A and amino acid residue 388 from subunit B.

While the enzyme was crystallized in the presence of 5PAH (Figure 1), a strong inhibitor of isomerase catalytic activity (*16*), the shape of the electron density map suggests a smaller compound is bound in each enzyme active site. An electron density map contains clear and connected electron density for all of the inhibitor molecule except for the hydroxyl group that is bound to the nitrogen atom in 5PAH (Figure 2, panel A). There is clear spherical density that is the appropriate size for an oxygen atom located near the nitrogen atom of the inhibitor, but the position of the density is such that an atom placed at the center of that sphere is too far away (2.5 Å) from the nitrogen atom to make a covalent bond with the nitrogen. In the crystal structure of triosephosphate isomerase complexed with phosphoglycolohydroxamate (*25*), the C−N distance is 1.40 Å. Furthermore, ab initio calculations of the hydroxamate function [R−C(O^-)═N−OH] give a value of 1.40 Å (work in progress). Instead of a covalently attached hydroxyl group, the density in the PGI/5PAH complex structure appears to be due to an ordered water molecule forming a hydrogen bond to an oxygen in the inhibitor, and it has been modeled as Water819.

The 5PAH inhibitor is likely to have been hydrolyzed during the several weeks between setting up the crystallization experiment and X-ray data collection. From the electron density map, it cannot be determined if the hydrolysis resulted in replacement of the nitrogen atom with an oxygen atom. Instead of the 5PAH molecule that was initially added to the crystallization solution, the bound compound appears to be 5-phospho-D-arabinonate (5PAA, Figure 1). Hydrolysis of 5PAH to produce 5PAA has been reported previously (*16*). Like the original compound, 5PAH, 5PAA is also an excellent inhibitor of the isomerase reaction (5PAH $K_i = 2 \times 10^{-7}$, 5PAA $K_i = 2 \times 10^{-6}$ M) (*19*, *26*) and mimic of the proposed intermediate of the reaction.

Interactions between the Inhibitor and the Enzyme. The 5PAA inhibitor is bound in a similar orientation as the 6PGA inhibitor in the previously reported rabbit PGI structure, but some of the interactions between the inhibitor and the active site amino acid residues vary. The new interactions are due to differences in the 6PGA and 5PAA molecules and to a conformational change in the enzyme. In addition, the use of high-resolution X-ray diffraction data (1.9 Å resolution) aided in the identification of additional ordered water molecules.

Overall, the active site pocket contains many more hydrogen bonding interactions than previously described (Figure 2, panel B). There is an extensive network of hydrogen bonds between the inhibitor, active site amino acids, and ordered water molecules that fills the active site pocket.

Conformational Change. A comparison of the 6PGA and 5PAA bound forms of the rabbit PGI enzyme identifies a small conformational change on one side of the active site pocket. The helix containing amino acid residues 513 to 522 is shifted toward the inhibitor (Figure 3). This new position brings Lys518 and Glu515 closer to the inhibitor. The side chain of Glu515 interacts with Water832, which forms hydrogen bonds with Oϵ1 of the inhibitor, the side chain of Lys518, and Water833. The side chain of Glu515 also makes hydrogen bonds with Waters 838 and 247 in the active site pocket. Water838 forms a hydrogen bond to Water860, which forms a hydrogen bond to Water833, which in turn interacts with Water832 and the O3P of the inhibitor.

The side chain of Lys518 interacts directly with O4 (2.9 Å) and O5 (3.0 Å) of the inhibitor. These distances were 4.9 and 6.6 Å to the equivalent positions on the 6-phospho-D-gluconate inhibitor (O5 and O6 of 6PGA, respectively). Lys518 also forms hydrogen bonds with Waters 836 and 832. Water836 in turn forms hydrogen bonds with the side chains of Thr211 and Thr214. Water832 forms hydrogen bonds with the inhibitor Oϵ1 (equivalent to the hydroxyl group on C2 of the proposed *cis*-enediol intermediate) and Water833, which in turn forms a hydrogen bond to an oxygen on the phosphate group of the inhibitor (O3P).

Phosphate Binding Site. The phosphate group of the 5PAA inhibitor forms many of the same interactions with the enzyme as seen with the 6PGA inhibitor, and there are some additional interactions. The phosphate group of the inhibitor forms hydrogen bonds with the side chains of Ser159, Ser209, Thr211, and Thr214, and with backbone amide groups from residues Lys210 and Thr211. The phosphate group also interacts with water molecules 817, 833, and 816. Water817 is in turn hydrogen bonded to the side chain of Thr217, the amide nitrogen of Ile156, and the carbonyl oxygen of Ala208.

The location of the phosphate atom in the binding site of the rabbit PGI with 5PAA structure was confirmed using an electron density omit map calculated with coefficients of |Fo − Fc| with the inhibitor molecules omitted and drawn with a 10 σ contour level (Figure 2, panel A). At this high contour level, the electron density for the protein and most of the inhibitor is not visible, but the electron density surrounding the electron-rich phosphate atom is still visible as a sphere. However, the orientation of the 5PAA molecule in the active site of the rabbit PGI differs from the orientation of the 5PAA in a structure of the *B. stearothermophilus* PGI reported during preparation of this paper. Chou and co-workers reported two structures of *B. stearothermophilus* PGI with bound competitive inhibitors 5PAA and *N*-bromoacetyl-

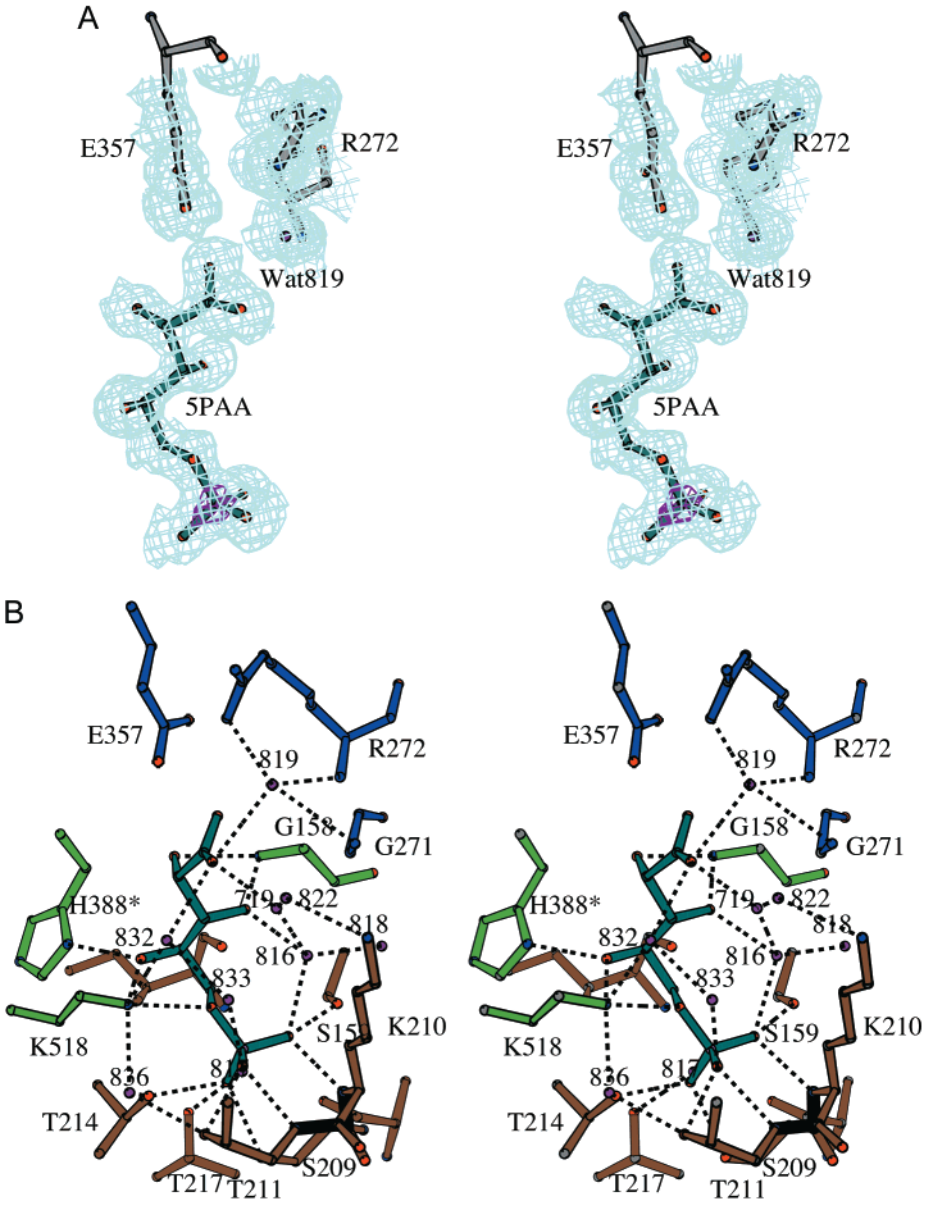

FIGURE 2: Isomerase Active Site. (A**)** Electron density maps. Part of an electron density map surrounding the 5PAA inhibitor and active site amino acid residues R272 and E357 is shown. An electron density map was calculated with coefficients of |2Fo − Fc| and shown with a 1 σ contour level (blue). An omit electron density map was prepared by leaving out the inhibitor molecule. The omit map was calculated with coefficients of |Fo − Fc| and is shown with a 10 σ contour level to indicate the position of the phosphate atom (purple) (*34*). (B) Stereo diagram of the active site. A ball-and-stick diagram of the 5PAA inhibitor is shown (dark green bonds) relative to essential amino acid residues of the active site and ordered water molecules (purple). Hydrogen bond interactions are indicated by dashed lines. Amino acids involved in binding the phosphate group are shown with orange bonds. Amino acids shown with light green bonds interact with C2-OH, C3-OH, or C4-OH (corresponding to substrate C3-OH, C4-OH, and C5-OH, respectively) and are likely to be involved in substrate specificity and in positioning the C1 end of the substrate close to residue Glu357. Amino acids shown with dark blue bonds are likely to be involved in proton transfer between C2 and C1 (Glu357), stabilization of the *cis*-enediol(ate) intermediate (Arg272, Gly271, Lys210), or positioning of the catalytic Glu357 side chain (Gln353). This figure and Figure 3 were made using the program MOLSCRIPT (*35*).

ethanolamine phosphate (*15*). In the bacterial PGI + bromoacetylethanolamine phosphate structure, the phosphate group of the inhibitor was located in a similar position to the phosphate group in the 5PAA or 6PGA inhibitors bound to the rabbit PGI, so that it forms hydrogen bonds with residues Ser140, Thr143, Glu417, and Lys420 (equivalent to Thr211, Thr214, Glu515, and Lys518, respectively, in rabbit PGI). However, in the structure of the *B. stearothermophilus* PGI with bound 5PAA inhibitor, the inhibitor was found to be turned around in the active site relative to the positioning of the 5PAA or 6PGA inhibitors in the rabbit PGI structures and the bromoacetylethanolamine phosphate inhibitor in the other bacterial PGI structure. In the bacterial PGI structure, the phosphate group of the 5PAA inhibitor forms hydrogen bonds with residues Gly201, Arg202, Glu285, and Gln413 (equivalent to residues Gly271, Arg272, Glu357, and Gln511 in rabbit PGI). One possible explanation for the two different binding orientations for the inhibitors in the two bacterial PGI structures is that the bacterial enzyme was crystallized in the presence of 50 mM inorganic phosphate. Inorganic phosphate is a weak competitive inhibitor of the isomerase reaction (K_i = 50 mM) (*9*). It is possible that inorganic phosphate competed with the phosphate group of the 5PAA inhibitor for the phosphate binding site and thereby prevented

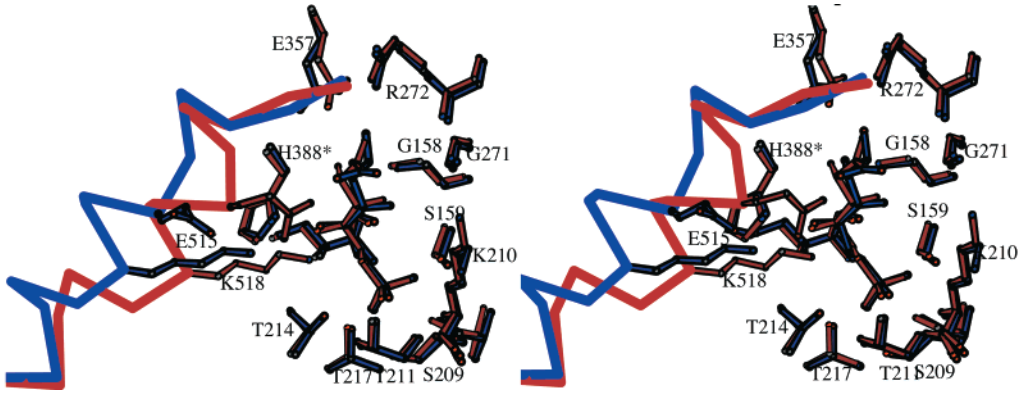

FIGURE 3: Stereo diagram of overlay of rabbit PGI with 5PAA and rabbit PGI with 6PGA. The α carbon atoms of residues 100−450 of the rabbit PGI structure with bound 6-phosphogluconate were superposed on the rabbit PGI structure with bound 5PAA, using the lsq_explicit command in the program O (*22*). A portion of the active site of the overlayed structures is shown as a stereo diagram with the PGI + 5PAA structure in red and the PGI + 6PGA structure in blue. Most of the amino acids are from one subunit in the dimer, except for His388, which is from the other subunit (indicated by the asterisk). Ball and stick models indicate the relative positions of several active site amino acid residues. The helix containing residues 513 to 522 is shown as an α-carbon trace to indicate the portion of the helix that has changed position. Most of the active site residues overlay quite closely. Exceptions include K518 and E515, which are in the helix that moved closer to the inhibitor. (OE1 and OE2 of the inhibitor correspond to Oϵ1 and Oϵ2 in the text.)

the 5PAA inhibitor from binding in the correct orientation in the crystal structure of the bacterial PGI.

Because of the considerable binding energy provided by the many interactions between the phosphate group of the 5PAA and 6PGA inhibitors in the rabbit structures (here and in ref *14*), which were determined in the absence of added inorganic phosphate, it is likely that the position of the phosphate group in the two crystal structures for the rabbit enzyme represent the binding orientation of the phosphate group of the substrate in the enzyme active site.

Substrate Specificity. The hydroxyl groups bound to C2, C3, and C4 of 5PAA (equivalent to the C3, C4, and C5 positions of G6P) also make several interactions with the enzyme. OH2 forms hydrogen bonds to the carbonyl oxygen of His388 and the amide nitrogen of Gly158. OH3 forms hydrogen bonds to the amide nitrogen of Gly158 and Water816. Water816 in turn forms hydrogen bonds to the inhibitor phosphate group and to two other water molecules in the hydrogen bonding network. OH4 forms hydrogen bonds with the side chains of His388 and Lys518. OH5 also forms a hydrogen bond with the side chain of Lys518.

These additional interactions between the enzyme and the inhibitor help explain the enzyme's strict specificity for glucose-6-phosphate and fructose-6-phosphate. While it appears that the numerous interactions between the phosphate group and the enzyme provide a firm anchor for binding one end of the substrate molecule to the enzyme, it is possible that additional interactions between the enzyme and the hydroxyl groups on the C3, C4, and C5 positions of the substrate help to position carefully C1 and C2 near the enzyme's catalytic residue(s). It is possible that the hydroxyl groups on other six-carbon sugars would not be in the correct positions to interact with the amino acid residues in the correct orientations, so the C1 and C2 positions of these other sugars would not be correctly positioned relative to the catalytic residues.

Mechanism of Reaction. Since 5PAA is likely to be a better mimic of the *cis*-enediol(ate) intermediate than 6PGA, the interactions between 5PAA provide a better indication of the interactions between the G6P substrate and the enzyme. Phosphoglucose isomerase has been extensively characterized biochemically. Its catalysis is believed to involve general acid/base catalysis with proton transfer via a 1,2-*cis*-enediol(ate) intermediate (*6*, *7*). In a proposed mechanism, the cyclic form of D-glucose-6-phosphate first binds to the active site. An acidic amino acid side chain from the enzyme protonates the ring oxygen and a basic side chain deprotonates the hydroxyl group at C1, promoting an electron shift that opens the ring. An enzymic base abstracts the C2 proton, and a double bond is formed between C1 and C2, yielding the *cis*-enediol(ate) intermediate. Then the enzymic base transfers the same proton back to the intermediate at C1, and concurrent electron shifts result in the loss of a proton from the oxygen at C2 and the gain of a proton by the oxygen at C1 of the substrate, resulting in the formation of the open-chain form of the product, D-fructose-6-phosphate. The cyclic form of D-fructose-6-phosphate can then be formed by transfer of a pair of electrons from the incipient ring oxygen to C2. Upon formation of this bond, the ketose oxygen accepts a proton from the protonated basic side chain.

pH profile experiments suggest that groups with pK_a's of 6.7 and 9.4, possibly a histidine and a lysine, are candidates for catalytic residues (*9*). In addition, chemical modification studies have also predicted that a histidine (*27*) and lysine (*28*) as well as glutamate (*29*), and arginine (*30*) residues are involved in the reaction. When the structure of rabbit PGI was determined with bound 6PGA, the presence of His388 and Lys518 in the active site pocket suggested that they would be good candidates for amino acid residues that promote transfer of a proton from C2 to C1. In the PGI with 6-phospho-D-gluconate structure, the C1 and C2 positions of the inhibitor were not located close to these two residues, but a possible explanation was presented that the true substrate could bind in a bent conformation to bring C1 and C2 closer to His388 and Lys518. However, in light of the new rabbit PGI structure containing 5PAA, a compound somewhat closer to the structure of the proposed *cis*-enediol(ate) intermediate, it appears that this model should be revisited with the possibility that other residues could also be involved in the transfer of a proton from C2 to C1. His388 and Lys518 could have other roles in the interaction with the substrate, such as in catalyzing ring opening. In Figure

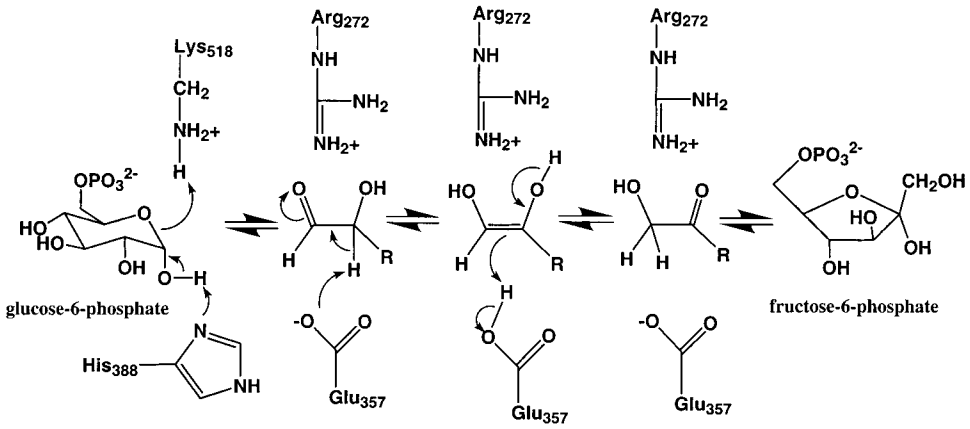

FIGURE 4: Proposed role of Glu357 in catalytic mechanism of PGI. First, His388 and Lys518 catalyze ring opening to yield the open chain form of D-glucose-6-phosphate. Lys518 protonates the ring oxygen, while His388 abstracts a proton from the hydroxyl group on C1. Then, the side chain of Glu357 abstracts a proton from the C2 position of the open chain form of the substrate, resulting in the *cis*-enediol(ate) intermediate. The protonated Glu357 side chain then transfers the same proton to the C-1 position of the intermediate, yielding the open chain form of D-fructose-6-phosphate. Arg272 helps stabilize the charged transition state.

2, panel B, these two residues are interacting with the hydroxyl on C4 of the inhibitor, which would correspond to the ring-oxygen of the cyclic form of the substrate (or to the hydroxyl on C5 of the linear form of the substrate).

Possible Catalytic Residues. The 5PAA-C1 corresponds to C2 of the *cis*-enediol(ate) intermediate. Because of the symmetry of the carboxylate group and some differences between the compound in the active site and the proposed *cis*-enediol(ate) intermediate, there is the possibility that the 5PAA Oϵ1 or Oϵ2 could be in the position of C1 (Figure 2, panel C). This would suggest that Water819 or Water719 would approximate the position of the hydroxyl group at G6P-C1, respectively. Water719 is located 2.6 Å from Oϵ1 and also forms a hydrogen bond to water 822 (2.8 Å). Water822 also forms a hydrogen bond to Lys210 Nϵ (2.8 Å). Neither of these would serve as good candidates to transfer the proton from C2 to C1 during catalysis.

In contrast, if the 5PAA-Oϵ2 represents the C1 of the intermediate, then a candidate for an enzymic functional group to transfer the proton would be the side chain of Glu357 (Figure 4). Oϵ1 of Glu357 is 2.5 Å from the 5PAA atom corresponding to C1 of the intermediate. It is also 3.2 Å from the 5PAA atom corresponding to C2. The side chain of Arg272 and the backbone nitrogens of Arg272 and Gly271 are in position to help stabilize the negative charge of the intermediate.

On the basis of the results from the rabbit PGI/5PAA complex crystal structure, we propose the following catalytic mechanism for PGI: In the first step, G6P binds to the enzyme active site with its phosphate group interacting with Ser209, Ser159, Thr211, and Thr214. Lys518 protonates the ring oxygen and His388 accepts a proton from the hydroxyl group on C1 to catalyze opening of the hexose ring. Interactions between the hydroxyl groups at C3, C4, and C5 of the open chain form of the substrate with His388, Gly158, and Lys518 and a network of ordered water molecules held in position by other conserved active site amino acid residues help position C1 and C2 near Glu357. Glu357 accepts a proton from C2 of the substrate, and accompanying electron shifts result in the formation of the *cis*-enediol(ate) intermediate. The *cis*-enediol(ate) intermediate is stabilized in part by the side chain of Arg272. Glu357 then protonates the intermediate at C1 to yield the open chain form of F6P. A reversal of the ring opening step results in formation of the cyclic form of F6P.

A database search and sequence alignment using the program BLAST (*31*) found 129 phosphoglucose isomerase sequences. Glu357, Arg272, His388, and Lys518 were completely conserved in all the sequences.

The mechanism presented in Figure 4 for PGI is similar to the catalytic mechanism proposed for triosephosphate isomerase (TIM). Both mechanisms involve a glutamate amino acid residue (Glu165 in TIM) that transfers a proton from C2 to C1 of the substrate to form a *cis*-enediol(ate) intermediate (*32*, *33*). Also, PGI Arg272 is located where it can provide a positive charge to help stabilize the negative charges of the enediol(ate) intermediate, which is the role of a similarly positioned Lys12 in TIM.

The mechanism presented here differs significantly from a mechanism proposed based on the structure of *B. stearothermophilus* PGI (*15*). In that mechanism, Lys420 (equivalent to Lys518 in rabbit PGI) is proposed to act as a general base to catalyze ring opening. His306 (equivalent to His388) transfers a proton from C2 to C1 of the substrate to form the *cis*-enediol(ate) intermediate, while Glu285 (equivalent to Glu357) protonates the C1 carbonyl oxygen. In addition, Arg202 (equivalent to Arg272) stabilizes the negative charge on Glu285, while Lys420 helps stabilizes the *cis*-enediol(ate) intermediate. While the equivalent Lys, Glu, His, and Arg amino acid residues play important roles in both proposed mechanisms, the role of each amino acid differs in the two mechanisms. Most notably, the role of transferring the proton from C2 to C1 was assigned by Chou and co-workers to His306, but in our mechanism, that role is assigned to Glu357. As described above, this is due to a different orientation of binding of the 5PAA inhibitor in the two structures, which probably results from the presence of phosphate in the crystallization conditions for the bacterial enzyme.

Summary. The crystal structure of mammalian PGI with bound 5PAA inhibitor has been solved at 1.9 Å. The orientation of the inhibitor in the active site pocket is in agreement with a previous structure of rabbit PGI with bound 6PGA in that the phosphate group interacts with Ser159,

Ser209, Thr211, Thr214, and Lys210. The new structure predicts that amino acid residue Glu357 transfers a proton between C2 and C1 of the substrate during catalysis. Lys518 and His388 are likely to be involved catalyzing ring opening to provide the open chain form of the substrate. The 5PAA inhibitor in the new structure makes many additional interactions between with the enzyme and with ordered molecules in the active site pocket. These additional interactions are likely to be responsible for the enzyme's strict substrate specificity.

ACKNOWLEDGMENT

We thank the staff of BioCARS staff for support and assistance in data collection at APS Sector 14 at Argonne National Labs.

REFERENCES

1. Andersson, S. G., Zomorodipour, A., Andersson, J. O., Sicheritz-Ponten, T., Alsmark, U. C., Podowski, R. M., Naslund, A. K., Eriksson, A. S., Winkler, H. H., and Kurland, C. G. (1998) *Nature 396* (6707), 133−40.
2. Chaput, M., Claes, V., Portetelle, D., Cludts, I., Cravador, A., Burny, A., Gras, H., and Tartar, A. (1988) *Nature 332* (6163), 454−5.
3. Faik, P., Walker, J. I., Redmill, A. A., and Morgan, M. J. (1988) *Nature 332* (6163), 455−7.
4. Watanabe, H., Takehana, K., Date, M., Shinozaki, T., and Raz, A. (1996) *Cancer Res. 56* (13), 2960−3.
5. Xu, W., Seiter, K., Feldman, E., Ahmed, T., and Chiao, J. W. (1996) *Blood 87* (11), 4502−6.
6. Rose, I. A., and O'Connell, E. L. (1961) *J. Biol. Chem. 236* (12), 3086−92.
7. Rose, I. A. (1975) *Adv. Enzymol. Relat. Areas. Mol. Biol. 43*, 491−517.
8. Rose, I. A. (1981) *Philos. Trans. R Soc. Lond. B Biol. Sci. 293* (1063), 131−43.
9. Dyson, J. E., and Noltmann, E. A. (1968) *J. Biol. Chem. 243* (7), 1401−14.
10. Swenson, C. A., and Barker, R. (1971) *Biochemistry 10* (16), 3151−4.
11. Shaw, P. J., and Muirhead, H. (1977) *J. Mol. Biol. 109* (3), 475−85.
12. Achari, A., Marshall, S. E., Muirhead, H., Palmieri, R. H., and Noltmann, E. A. (1981) *Philos. Trans. R Soc. Lond. B Biol. Sci. 293* (1063), 145−57.
13. Sun, Y. J., Chou, C. C., Chen, W. S., Wu, R. T., Meng, M., and Hsiao, C. D. (1999) *Proc. Natl. Acad. Sci. U.S.A. 96* (10), 5412−7.
14. Jeffery, C. J., Bahnson, B. J., Chien, W., Ringe, D., and Petsko, G. A. (2000) *Biochemistry 39* (5), 955−64.
15. Chou, C. C., Sun, Y. J., Meng, M., and Hsiao, C. D. (2000) *J. Biol. Chem. 275* (30), 23154−60.
16. Hardré, R., Bonnette, C., Salmon, L., and Gaudemer, A. (1998) *Bioorg. Med. Chem. Lett. 8* (23), 3435−8.
17. Parr, C. W. (1956) *Nature 178*, 1401−1401.
18. Chirgwin, J. M., Parsons, T. F., and Noltmann, E. A. (1975) *J. Biol. Chem. 250* (18), 7277−9.
19. Hardré, R., and Salmon, L. (1999) *Carbohydr. Res. 318* (1−4), 110−5.
20. Otwinowski, Z., and Minor, W. (1997) *Processing of X-ray Diffraction Data Collected in Oscillation Mode*, in *Macromolecular Crystallography, Part A* (Carter, C. W., Jr., Sweet, R. M., Ed.) pp 307−26, Academic Press.
21. Brunger, A. T., Adams, P. D., Clore, G. M., DeLano, W. L., Gros, P., Grosse-Kunstleve, R. W., Jiang, J. S., Kuszewski, J., Nilges, M., Pannu, N. S., Read, R. J., Rice, L. M., Simonson, T., and Warren, G. L. (1998) *Acta Crystallogr. D Biol. Crystallogr. 54* (Pt5), 905−21.
22. Jones, T. A., Zou, J. Y., Cowan, S. W., and Kjeldgaard, M. (1991) *Acta Crystallogr. A 47* (2), 110−9.
23. Brunger, A. T. (1992) *Nature 355* (6359), 472−5.
24. Collaborative Computational Project, N. (1994) *Acta Crystallogr. D 50*, 760−3.
25. Zhang, Z., Komives, E. A., Sugio, S., Blacklow, S. C., Narayana, N., Xuong, N. H., Stock, A. M., Petsko, G. A., and Ringe, D. (1999) *Biochemistry 38* (14), 4389−97.
26. Chirgwin, J. M., and Noltman, E. A. (1975) *J. Biol. Chem. 250* (18), 7272−6.
27. Gibson, D. R., Gracy, R. W., and Hartman, F. C. (1980) *J. Biol. Chem. 255* (19), 9369−74.
28. Schnackerz, K. D., and Noltman, E. A. (1971) *Biochemistry 10* (26), 4837−43.
29. O'Connell, E. L., and Rose, I. A. (1973) *J. Biol. Chem. 248* (6), 2225−31.
30. Riordan, J. F., McElvany, K. D., and Borders, C. L., Jr. (1977) *Science 195* (4281), 884−6.
31. Altschul, S. F., Madden, T. L., Schaffer, A. A., Zhang, J., Zhang, Z., Miller, W., and Lipman, D. J. (1997) *Nucleic Acids Res. 25* (17), 3389−402.
32. Lolis, E., and Petsko, G. A. (1990) *Biochemistry 29* (28), 6619−25.
33. Straus, D., Raines, R., Kawashima, E., Knowles, J. R., and Gilbert, W. (1985) *Proc. Natl. Acad. Sci. U.S.A. 82* (8), 2272−6.
34. Esnouf, R. M. (1997) *J. Mol. Graphics 15* (2), 133−8.
35. Kraulis, P. J. (1991) *J. Appl. Crystallogr. 24*, 946−50.

BI0018483